Geomorphology 248 (2015) 237–251

Contents lists available at ScienceDirect

Geomorphology

journal homepage: www.elsevier.com/locate/geomorph

Plugs or flood-makers? The unstable landslide dams of eastern Oregon

E.B. Safran [a,*], J.E. O'Connor [b], L.L. Ely [c], P.K. House [d], G. Grant [e], K. Harrity [f,1], K. Croall [f,1], E. Jones [f,1]

[a] Environmental Studies Program, Lewis & Clark College, MSC 55, 0615 SW Palatine Hill Road, Portland, OR 97219, USA
[b] U.S. Geological Survey, Geology, Minerals, Energy, and Geophysics Science Center, 2130 SW 5th Avenue, Portland, OR 97201, USA
[c] Department of Geological Sciences, Central Washington University, Ellensburg, WA 98926, USA
[d] U.S. Geological Survey, Geology, Minerals, Energy, and Geophysics Science Center, 2255 N. Gemini Drive, Flagstaff, AZ 86001, USA
[e] U.S. Forest Service, Pacific Northwest Research Station, 3200 SW Jefferson Way, Corvallis, OR 97331, USA
[f] Lewis & Clark College, 0615 SW Palatine Hill Road, Portland, OR 97219, USA

ARTICLE INFO

Article history:
Received 25 November 2014
Received in revised form 26 June 2015
Accepted 26 June 2015
Available online 8 July 2015

Keywords:
Landslides
Landslide dams
Mass movements
Eastern Oregon
Geomorphology

ABSTRACT

Landslides into valley bottoms can affect longitudinal profiles of rivers, thereby influencing landscape evolution through base-level changes. Large landslides can hinder river incision by temporarily damming rivers, but catastrophic failure of landslide dams may generate large floods that could promote incision. Dam stability therefore strongly modulates the effects of landslide dams and might be expected to vary among geologic settings. Here, we investigate the morphometry, stability, and effects on adjacent channel profiles of 17 former and current landslide dams in eastern Oregon. Data on landslide dam dimensions, former impoundment size, and longitudinal profile form were obtained from digital elevation data constrained by field observations and aerial imagery; while evidence for catastrophic dam breaching was assessed in the field. The dry, primarily extensional terrain of low-gradient volcanic tablelands and basins contrasts with the tectonically active, mountainous landscapes more commonly associated with large landslides. All but one of the eastern Oregon landslide dams are ancient (likely of order 10^3 to 10^4 years old), and all but one has been breached. The portions of the Oregon landslide dams blocking channels are small relative to the area of their source landslide complexes (0.4–33.6 km^2). The multipronged landslides in eastern Oregon produce marginally smaller volume dams but affect much larger channels and impound more water than do landslide dams in mountainous settings. As a result, at least 14 of the 17 (82%) large landslide dams in our study area appear to have failed cataclysmically, producing large downstream floods now marked by boulder outwash, compared to a 40–70% failure rate for landslide dams in steep mountain environments. Morphometric indices of landslide dam stability calibrated in other environments were applied to the Oregon dams. Threshold values of the Blockage and Dimensionless Blockage Indices calibrated to worldwide data sets successfully separate dam sites in eastern Oregon that failed catastrophically from those that did not. Accumulated sediments upstream of about 50% of the dam sites indicate at least short-term persistence of landslide dams prior to eventual failure. Nevertheless, only three landslide dam remnants and one extant dam significantly elevate the modern river profile. We conclude that eastern Oregon's landslide dams are indeed floodmakers, but we lack clear evidence that they form lasting plugs.

1. Introduction

Rivers propagate climatic and tectonic signals through landscapes, creating local relief and setting the base level to which tributaries and hillslopes respond. Consequently, the longitudinal profile evolution of mainstem rivers may strongly regulate landscape response to external forcing (e.g., Whipple and Tucker, 1999), particularly in unglaciated landscapes and in landscapes affected by significant rates of uplift or base-level drop. In this conceptual framework, hillslopes are usually cast as responding passively to fluvial drivers. However, recent work has highlighted the ways in which hillslope–channel interactions can modulate local fluvial incision rates over timescales of 10^4–10^5 years (e.g., Hewitt, 1998, 2006; Korup, 2002; Ouimet et al., 2007; Korup et al., 2010; Burchsted et al., 2014). Particular attention has been paid to the effects of large, dam-forming landslides on river morphology and sediment storage over multiple spatial and temporal scales. For example, epicycles of aggradation upstream of landslide dams and incision through the deposits or adjacent bedrock dominate sediment deposition and erosion patterns over 10^3–10^4 years in parts of the Himalaya (e.g., Hewitt, 1998; Korup et al., 2006; Hewitt et al., 2008, 2011). A recent modeling study by van Gorp et al. (2014) likewise simulated impacts of landslide damming on sediment storage and release that persist for at least 15,000 years. The lag deposits and sediment wedges associated with long-lived landslide dams can also create persistent

* Corresponding author.
E-mail address: safran@lclark.edu (E.B. Safran).
[1] Former address.

http://dx.doi.org/10.1016/j.geomorph.2015.06.040
0169-555X/

knickpoints and associated alluvial plains (e.g., Korup, 2005, 2006, 2011; Schuster, 2006; Ouimet et al., 2007; Walsh et al., 2012), forming prominent morphologic features in some river valleys.

Landslides can affect the longitudinal profile evolution of rivers in two contrasting manners. Large landslides can inhibit incision locally by altering channel slope, width, and bed character and by burying the valley bottom under landslide material. Dam-forming landslides can also affect reaches upstream from the incursion site because fluvial incision ceases in the dam pool during the lifetime of the dam. If the dam is long-lived, sediment may accumulate in this reservoir, extending the timescale of longitudinal profile recovery until the sediment is evacuated (e.g., Hewitt, 1998). The persistent inhibition of incision in landslide-prone channel reaches, particularly in downstream-most reaches, would tend to produce local to regional convexities in the longitudinal profiles of rivers subject to external forcing (e.g., Ouimet et al., 2007; Safran et al., 2008).

By contrast, through natural dam failures, dam-forming landslides can generate cataclysmic floods (e.g., Costa and Schuster, 1988; Ermini and Casagli, 2002; O'Connor et al., 2003a, 2013) that have the potential to incise through valley fill or bedrock. These outburst floods can be much larger than meteorologically generated floods and can set the basic architecture of the channel for many thousands of years (Beebee, 2003; O'Connor and Grant, 2003; Schuster, 2006). The incision caused by individual outburst floods from other types of natural dams, such as ice dams, calderas, or tectonic basins, has been well documented (reviewed in O'Connor et al., 2013). Such dams typically impound larger water bodies than landslide dams, with a few notable exceptions (O'Connor et al., 2003a; O'Connor and Beebee, 2009); consequently we expect any enhanced incision during outburst floods from breached landslide dams to be more modest than for other types of outburst floods. However, in environments where landslide dams are spatially and temporally frequent and susceptible to failure, such effects could potentially be significant, especially where topographic or climatic conditions do not drive high background rates of incision.

Not all landslide dams fail catastrophically, however, and the question of whether or not landslide dams may cataclysmically breach has important implications for hillslope–channel coupling and controls on landscape evolution. This issue has been addressed in the context of natural hazards where some assessments of dam stability relate dam size to water available for dam breaching (Casagli and Ermini, 1999; Ermini and Casagli, 2003; Korup, 2004). Threshold values of morphometric functions, or indices, that partially distinguish between *stable* and *unstable* landslide dams have been determined for the Italian Apennines (Casagli and Ermini, 1999); for the New Zealand Southern Alps (Korup, 2004); for composite data sets predominantly from Italy, Japan, and the western U.S., with a smattering of examples from the Canadian Cordillera, New Zealand, and elsewhere (Ermini and Casagli, 2003); and for the Argentine Andes (Hermanns et al., 2006, 2011a). Dams that impound extant lakes or ancient lakes that filled with sediment have commonly been classified as *stable*, although extant lakes still have the potential to drain catastrophically through future dam failure. Costa and Schuster (1991), Hewitt (1998), Ermini and Casagli (2002), and Hermanns et al. (2006, 2011a) reported cases of catastrophic failure after hundreds or even thousands of years of dam persistence, e.g., caused by landsliding into existing landslide-dammed lakes and changes in climatic conditions (e.g., Hermanns et al., 2006, 2011a). The *unstable* landslide dam classification has sometimes been used to denote catastrophic breaching (e.g., Ermini and Casagli, 2003; Hermanns et al., 2011a), but in many instances breaching occurs in an unspecified manner, and stability classifications are ambiguous (e.g., Korup, 2004; Hermanns et al., 2011a). Here, we do not attempt to designate *stable* landslide dams but rather focus on whether dams in our study area failed catastrophically or not.

Dam stability analyses have predominantly been applied in rugged, mountainous terrain. However, the propensity for landslide dams to fail catastrophically — and associated consequences for channels — likely varies across geologic settings, because of differences in regional physiography, landslide distribution, or landslide type. Some lower-relief environments also exhibit widespread landsliding (e.g., Reneau and Dethier, 1996; Philip and Ritz, 1999; Korup et al., 2007; Safran et al., 2011), but the stability of landslide dams in such settings has not been analyzed.

To address that gap and better understand the formation, failure, and geomorphic consequences of landslide dams in a different environment, we analyze the history and morphometry of 17 ancient landslide dams and their adjacent channels in eastern Oregon. We compare these landslide dam characteristics with two other data sets summarizing landslide dam characteristics from New Zealand (Korup, 2004) and select worldwide sites (Ermini and Casagli, 2003; Korup, 2004). We evaluate field evidence for catastrophic failure, as well as field and map evidence of effects of landsliding on longitudinal river profiles. For each landslide dam, we then compute the value of five stability indices (Blockage index, Dimensionless Blockage index, Impoundment index, Backstow index, Basin index; Ermini and Casagli, 2002, 2003; Korup, 2004). We assess whether any previously published threshold values of these stability indices, derived from other environments, are consistent with our own field observations relating to dam failure. Our primary aim is to contribute to a more complete picture of the character and behavior of landslide dams by providing data from one of the least tectonically active landscapes likely to support many large landslide complexes, which is important for understanding the diverse potential long-term effects of large landslides on channel and landscape evolution. Our secondary aim is to probe the utility of dam-stability indices and their calibrated failure-threshold values as an interpretive framework for making such comparisons across geologic environments (e.g., Korup, 2004; Hermanns et al., 2006, 2011a).

2. Study area and dam sites

The sites selected for this study lie east of the Cascade Range within the Deschutes, John Day, Malheur, and Owyhee river basins of eastern Oregon (Fig. 1).

This semiarid landscape lies in the rain shadow of the Cascade Range and receives on average 25–38 cm of rain/y, with local maxima of 50–75 cm/y in the Ochoco and Strawberry Mountains. The regional geology consists primarily of volcanic and volcaniclastic rocks of Tertiary and Quaternary age. Thick sequences of fluviolacustrine sediments have accumulated since the Miocene in tectonically controlled, largely extensional basins (Cummings, 1991; Christiansen and Yeats, 1992; Cummings et al., 2000). Igneous deposits ranging in composition from rhyolitic ash flow tuffs and calderas to basaltic lava flows form low-gradient plateau tops punctuated by higher-standing peaks. The region stands at an elevation of >1 km above mean sea level (amsl), rising to an average surface elevation of almost 1.4 km amsl near the shared borders of Oregon, Idaho, and Nevada (Camp and Ross, 2004). The uplifted plateaus are dissected by canyons cut by major rivers, creating corridors where local relief reaches a few 100 m (Fig. 2).

Most large rivers in this region drain to either the Snake or Columbia rivers. Modest local relief was likely already established in the mid- to late-Pliocene, in part caused by capture of the Snake River by the Columbia River ~3–4 Ma (Repenning et al., 1995; Van Tassell et al., 2001) and in part because of other, incompletely understood drivers. Average incision rates on the Deschutes River, a tributary of the Columbia River, were about 0.1 mm/y between ~4 and 1 Ma, when the river reached its near-present level (O'Connor et al., 2003b). In the last ~2 Ma, long-term incision rates on the Owyhee River (a tributary to the Snake River) between Rome and Birch Creek have been ~0.2 mm/y (Ely et al., 2012). Although the regional drainage pattern was broadly established by middle Miocene to early Pliocene times (Smith, 1986; Beranek et al., 2006), the combination of low precipitation rates, low regional gradients, and tectonic and volcanic disruption of drainage networks has led to poor hydrologic integration. Nearly 60,000 km^2 of

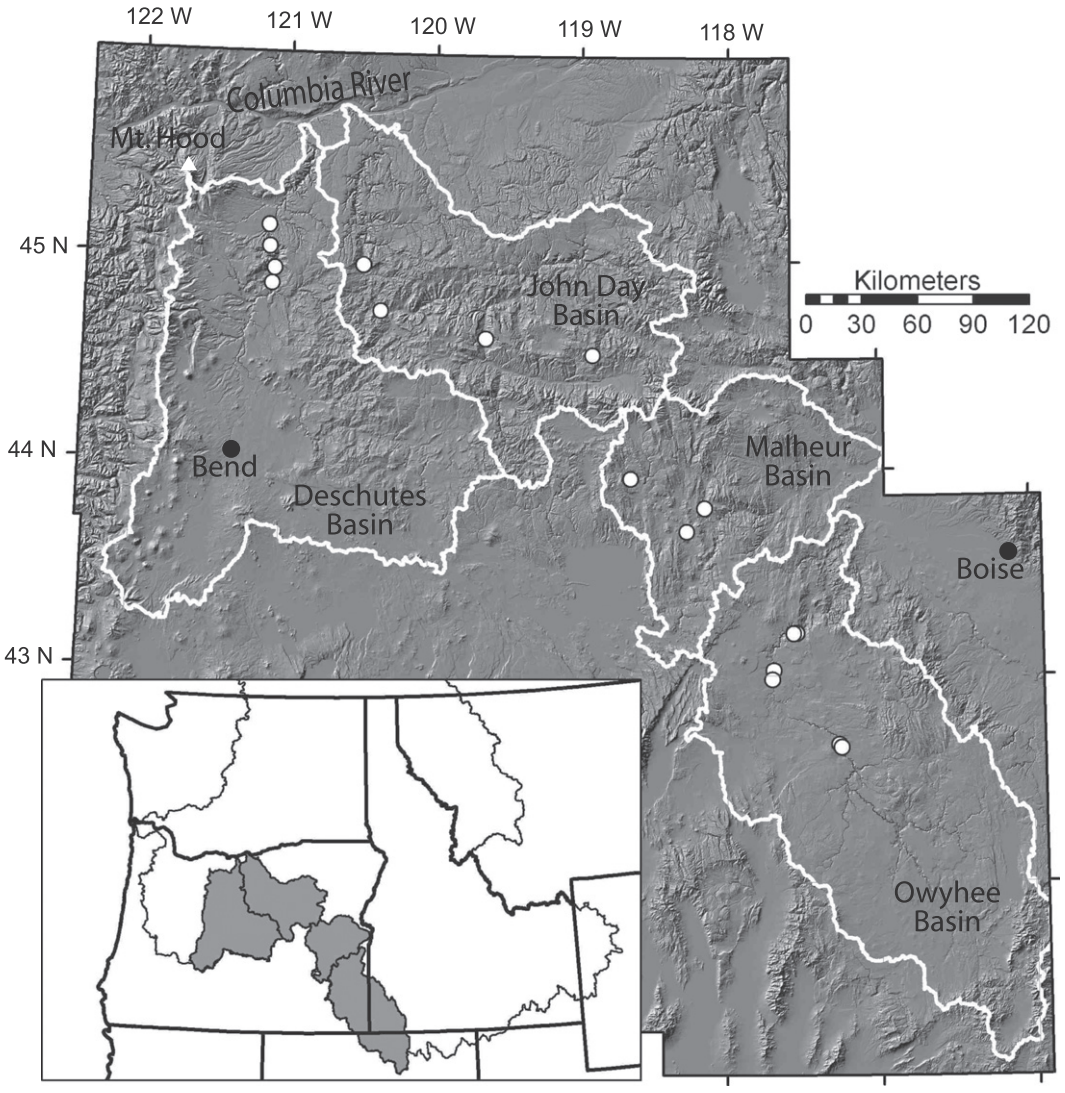

Fig. 1. Location map of landslide dam sites analyzed. Thin black outline in inset map depicts Columbia River basin boundary.

eastern Oregon is presently internally drained, although portions of those areas were integrated during wetter climatic times (Carter et al., 2006).

Large landslide complexes, some larger than 30 km^2, are widespread throughout the region (Safran et al., 2011). Their distribution is preferentially associated with escarpments where coherent volcanic rock units overlie weak, volcaniclastic debris with several tens to hundreds of meters of local relief (Safran et al., 2011). The spatial density of mapped faults exerts no control on landslide distribution, while about 10% of landslides occur within 3–10 km of mapped fold axes

Fig. 2. View of Owyhee River illustrating typical regional landscape morphology. Tertiary and Quaternary lava flows form plateaus at multiple elevations, and incising river canyons create local relief of several 100 m.

(Safran et al., 2011). Most of the >400 landslides that have been mapped throughout the region are multiple rotational slides, but ~5–10% are earth flows, debris flows, and lateral spreads (Safran et al., 2011). Geochronologic constraints are weak and are available for only ~5% of mapped complexes, but they indicate that some are at least as young as early Holocene age, while most are likely Pleistocene (Safran et al., 2011). The age of the landslides and the lack of spatial association with faults suggests that triggers may have been climatic, primarily restricted to periods of greater moisture availability. Although precipitation rates at the last glacial maximum were likely approximately the same as today's (Oster et al., 2015), reduced evaporation rates led to the formation of lakes in some of the closed basins of eastern Oregon and the Great Basin (Ibarra et al., 2014), suggesting a net increase in terrestrial moisture. These conditions could have promoted landsliding during the Pleistocene.

Many landslides in eastern Oregon are known or are strongly suspected to have blocked rivers in the past (Beebee, 2003; O'Connor et al., 2003a; Othus, 2008; Safran et al., 2011), but we are aware of only one landslide in the region that still impounds a lake. All other blockages have been breached. A similar situation was faced by Hermanns et al. (2006) in the NW Argentinian Andes; but in other regions where landslide dams have been studied, samples of intact and of breached landslide dams exist (Casagli and Ermini, 1999; Ermini and Casagli, 2003; Korup, 2004; Hermanns et al., 2011a). In eastern Oregon, we relied on field observations of dam remnants and the surrounding channel reaches to assess evidence for catastrophic breaching or persistence.

The landslide sites selected for the present study constitute only a small subset of mapped landslides that may have blocked the region's rivers. The sites were selected because of clear evidence for channel blockage and/or good preservation of the morphology of the landslide dam. Several sites from each major drainage basin were selected, and the sites represent the diversity of landslide types in the region (Table 1). We have made field visits to all but three of the dam sites. Some form of geochronologic constraint on the age of the landslides, landslide dams, or outburst floods exist for almost half of the sites, described below.

3. Geochronologic constraints on landslide dams

Most geochronologic information about the eastern Oregon landslide dams is indirect and relates either to the landslides or to associated outburst floods; dated sediment accumulations upstream of landslide dams are rare. In the Deschutes River basin, age constraints on the Whitehorse landslide dam are weak; the slide occurred sometime between 38,740 ± 540 ^{14}C YBP and the 7.7 ka Mazama eruption (O'Connor et al., 2003a). Sediments inferred to have been deposited in an impoundment upstream of the Dant debris flow contain pumice granules similar to ones from the same area dated at 0.40–0.46 Ma (O'Connor et al., 2003a). Auger holes dug into sediments collected in closed depressions on the Wapinitia landslide and the morphologically fresher-looking Boxcar landslide downstream indicate the presence of the 7.7 ka Mt. Mazama ash. The ash is at the base of the sediments on the Boxcar landslide and close to, but not at, the base of the sediments on the Wapinitia landslide, consistent with the relative age assessment based on morphology. In the John Day River basin, the Magone Lake site affords the only direct indication of time of dam formation, supposedly in the late 1800s (Mosgrove, 1980). Mazama ash was found in a closed depression on the Burnt Ranch landslide toe, implying that this landslide also pre-dates the Mazama eruption. In the Malheur River basin, widespread tephra from the Mt. Mazama eruption of 7.7 ka is absent in the prominent bank cuts in sediment accumulations upstream of the Chukar Park site, suggesting a post-Mazama age for the landslide blockage. In the Owyhee River basin, the most recent blockage of the river in the reach of the Artillery landslide complex was most likely between 28 ± 2 and 18 ± 1 ka, based on ^{3}He cosmogenic radionuclide (CRN) ages of outburst flood boulders directly downstream. The age of the East Springs Greeley earth flow is not well constrained. Mazama tephra (7.7 ka) was found in a closed depression on the large boulder bar immediately downstream, which could be an outburst flood deposit from this earth flow blockage. Two ^{3}He CRN samples yielded ages of 354 ± 25 ka on the uppermost portion of the boulder bar and 14 ± 1 ka on a lower portion. Based on the landslide's well-preserved morphology, the age is most likely closer to the younger end of this range. No geochronologic information exists for the Hogsback site, but morphologically it is one of the most rugged landslides along the Owyhee corridor. Based on comparison with other landslides along this river for which we do have some age information (Safran et al., 2011), it is likely less than ~10 ka.

4. Dam and reservoir morphometry

4.1. Methods

As noted by Korup (2004), acquisition of morphometric data for landslide dams is a difficult task that includes many subjective judgments. Methodological detail about these judgments is often lacking in the literature, hindering comparisons among studies. Therefore, only major differences among landslide dam populations documented by different researchers are likely to be credible. Here we describe how we determined the values of seven parameters that are either reported as summary statistics of other landslide-dam samples or used to compute various dam stability indices (Ermini and Casagli, 2002, 2003; Korup, 2004). We also describe the collection of longitudinal profile data used to assess the long-term effects of the landslide dams.

Former channel blockages were identified using one or more key criteria, which were assessed either in the field, remotely, or both. Criteria included i) observation of an individual landslide deposit on both sides of the present-day stream (e.g., Fig. 3A); ii) highly constricted and/or laterally displaced river reaches (e.g., Fig. 3B); iii) the presence of rapids in the constricted reach, suggesting a lag deposit; iv) terraces upstream of potential blockages at or below the probable dam height, suggesting sediment accumulation within the impoundment; or v) outburst deposits downstream of the blockage, such as boulder bars or flood-swept boulders on elevated surfaces. Remote assessments of these features were made using Google Earth imagery, 1-m resolution color orthophoto quarter quadrangles of National Agricultural Inventory Project (NAIP) imagery, 10-m digital elevation models (DEMs), and where available (for reaches of the Owyhee and Deschutes rivers), higher-resolution DEMs derived from lidar data.

For each landslide dam, we identified a critical site cross section and the breach zone defining the effective along-channel extent of the dam (W_D; note that we adhere to the standard though the convention is confusing: that landslide dam width is defined in the along-channel direction and dam length (L_D) is defined in the cross-channel direction; Costa and Schuster, 1988). These were digitized as line features into shapefiles (Supplementary data Repository items 1 and 2); examples are shown in Fig. 4.

The critical cross section was located at the point of maximum channel constriction or at the location where the height of the landslide dam (H_D) was determined. The height of the landslide dam was defined by the lowest point of the critical cross section subtracted from the elevation of field-identified overflow features on or adjacent to the landslide, indicating a spillover elevation (e.g., Wapinitia, Warm Springs Reservoir, East Springs Greeley); the maximum elevation of backwater sediment deposits (*Dant*); or in the majority of cases, as the elevation of the minimum alternative spillover (MAS) route (Fig. 4). The MAS defines the location along the critical cross section where water impounded behind the dam would have spilled if it had not carved down at the present channel location. It represents a local elevation minimum, apart from the present channel, along the critical section.

Table 1
Eastern Oregon landslide dam sites analyzed in this study.

Site name	Major river basin	Long. (decimal degrees)	Lat. (decimal degrees)	Landslide complex area (km^2)	Landslide type	Evidence for blockage and persistence/failure	Drainage area upstream of blockage (km^2)	Landslide dam height/length/width (m)			Lake vol. (m^3)	Lake length (m)
Whitehorse	Deschutes	121.0782	44.9393	7.1	Complex rotational failure	Terraces upstream, boulder bars downstream	24,645	45	359	950	2.09×10^8	2.13×10^4
Dant	Deschutes	121.1154	45.0440	0.4	Debris flow	Lake sediments upstream, boulder lag downstream	24,827	30	166	560	3.74×10^7	1.31×10^4
Wapinitia	Deschutes	121.1240	45.1473	0.7	Complex rotational failure		25,164	19	206	400	7.39×10^6	7.99×10^3
Warm Springs River	Deschutes	121.0936	44.8651	1.1	Debris flow		1401	30	195	275	1.09×10^7	6.50×10^3
Magone Lake	John Day	118.9144	44.5460	0.4	Rock avalanche?	Extant lake	3	6	100	390	ND[a]	8.75×10^2
Sheep Rock	John Day	119.6382	44.6210	9.7	Complex rotational failure	Suspected lake sediments upstream, flood torrent terrace downstream	5292	37	367	550	5.32×10^7	1.08×10^4
Burnt Ranch	John Day	120.3533	44.7436	3.2	Earth flow	Terraces upstream, boulder bars and elevated gravel deposits downstream	14,567	33	289	500	9.62×10^7	2.15×10^4
Clarno	John Day	120.4770	44.9668	33.6	Complex rotational failure	Flood swept boulders on downstream end of dam	15,533	32	379	860	1.53×10^8	2.52×10^4
Wolf Creek	Malheur	118.6523	43.9491	11.3	Earth spread	Extensive gravel accumulation upstream	341	54	447	3280	1.21×10^8	6.80×10^3
Warm Springs Reservoir	Malheur	118.2752	43.6963	39.6	Earth spread	Boulder bars downstream	2530	9	84	350	2.21×10^6	4.41×10^3
Chukar Park	Malheur	118.1584	43.8109	2.4	Complex rotational failure	Sediment accumulation and change in river morphology upstream, boulder bars downstream	1235	52	368	1500	7.02×10^7	1.02×10^4
Hogsback	Owyhee	117.2550	42.6546	1.2	Complex rotational failure		15,166	23	172	660	3.58×10^6	6.16×10^3
Deary Pasture	Owyhee	117.2684	42.6670	1.2	Complex rotational failure	Flood swept boulders downstream of blockage	15,169	53	210	525	2.83×10^7	1.49×10^4
Heaven's Gate	Owyhee	117.7075	42.9808	0.8	Complex rotational failure	Boulder bar downstream	22,951	52	344	460	8.02×10^7	2.97×10^4
Artillery	Owyhee	117.6989	43.0271	1.1	Complex rotational failure	Boulder bar downstream	23,072	37	341	200	2.32×10^7	1.26×10^4
West Springs Greeley	Owyhee	117.5658	43.2053	7.9	Earth flow	Possible related terraces upstream	25,145	28	300	1920	2.39×10^7	8.21×10^3
East Springs Greeley	Owyhee	117.5478	43.2071	2.9	Earth flow	Boulder bar downstream, possible related terraces upstream	25,157	36	219	710	2.68×10^7	7.37×10^3

[a] ND = no data.

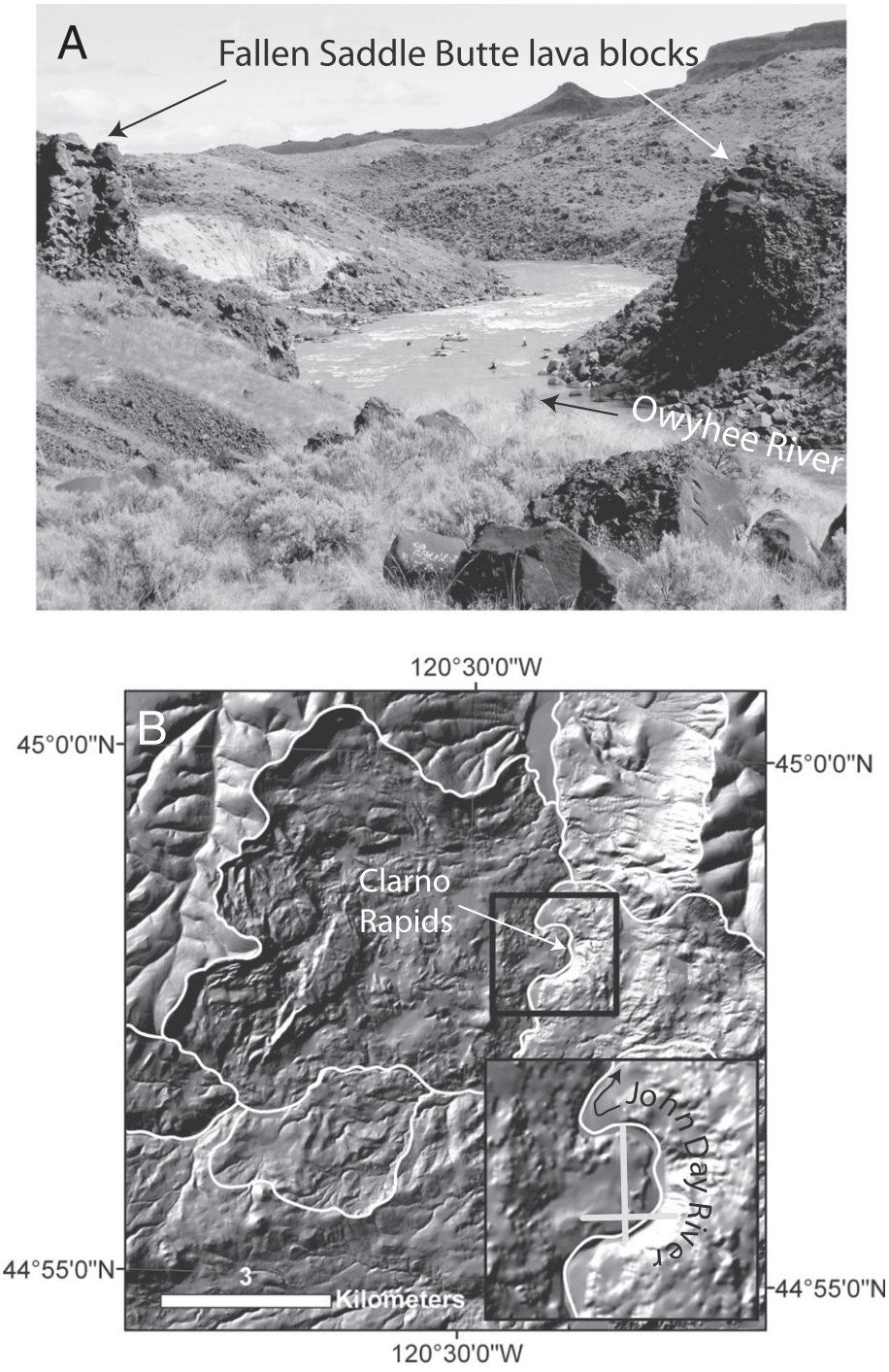

Fig. 3. Example indicators of former channel blockages. (A) Landslide deposits that span the present-day channel. At the Artillery site on the Owyhee River, the Saddle Butte lava flow is in place only on the western (left) side of the river. However, large blocks of Saddle Butte lava involved in a complex rotational failure are found on both sides of the river, indicating that the landslide deposit must have previously blocked the river. Rafters in center of photo for scale. (B) Sharp local deflections of the basal stream. A finger of material ~0.6 km^2 within the ~33 km^2 Clarno landslide complex has pushed the John Day River eastward, causing undercutting and steepening of the eastern (right) side of the valley. A sag pond on the protrusion and rapids in the adjacent channel reach, interpreted as a lag deposit, provide further evidence of a breached landslide dam. Gray lines in inset map show cross section used to determine dam height (horizontal line) and presumed length of breach zone (vertical line). Background image is a shaded relief rendering of a 10-m-resolution digital elevation model.

The elevation of the MAS therefore represents a maximum possible landslide dam height.

The extent of the breach zone (W_D) was determined by the extent of associated landforms: channel constrictions, rapids, or the start or end points of outburst flood bars or upstream sediment accumulations, respectively. The length of the landslide dam (L_D) across the channel was more difficult to identify, particularly at locations where there were multiple landslide complexes on both sides of the present channel (e.g., Fig. 3B). In such cases, the blocking sections of the landslides do not appear as distinct invasions of a well-defined valley floor, such as those formed by rock avalanches in steep mountain valleys. The valley walls themselves are landslide masses, and the channel weaves its way among and through the failed blocks. For this reason, we defined the across-channel length of the dam as the length of failure mass in contact with the reservoir impounded by the chosen dam height at the critical dam cross section (see below; Fig. 4). This is the across-channel extent

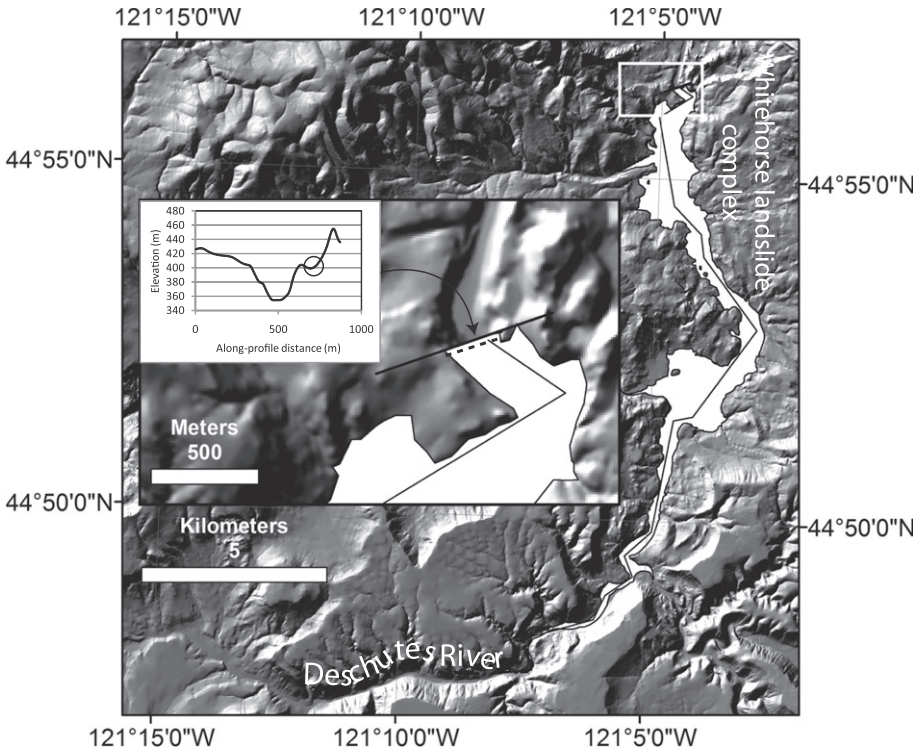

Fig. 4. Illustration of GIS features used to characterize landslide dam and impoundment morphologies; Whitehorse landslide dam on Deschutes River. White color indicates extent of the reservoir impoundment associated with landslide dam height determined by identifying minimum alternative spillover elevation (Section 4.1). Solid line along reservoir was used to determine reservoir length. Inset shows close-up of dam site and valley cross section at the dam location indicated by the solid black line on the main map. Elevation and location of alternative minimum spillover route circled on cross-sectional profile. Dashed line indicates dam length used in morphometric analyses.

of material that was involved in holding back the water impounded by the dam.

The volume and length of the lake (V_L and L_L, respectively) impounded by a landslide dam were determined as follows. Once H_D was identified and the critical dam cross section located, a smaller DEM extending upstream from the dam site and up the valley walls from the blocked channel was extracted from the base DEM. A raster data set delineating elevations less than or equal to that of H_D was determined from this smaller DEM. This data set defined the planview pattern of the reservoir that would have formed behind the dam (Fig. 4). Care was taken to ensure that the smaller DEM neither cut off places to which the reservoir would have otherwise extended nor included water bodies separate from the reservoir. A line was digitized along the generalized path of the reservoir to define the length of the lake (Fig. 4; Supplementary data Repository item 3). The volume of the reservoir was computed using the Area and Volume tool in 3D Analyst of ESRI ArcGIS. The H_D was used as the threshold elevation, and the volume beneath that plane was computed using the small DEM. This method by necessity assumes that the modern topography existed at the time that the landslide dam was emplaced. Computed volumes could be underestimates if significant sedimentation occurred in the valley while or after the dam was in place. Computed volumes could also be overestimates if large landslides developed subsequent to the dam, broadening the valley and creating more space for impounded water than existed during the dam's lifetime. Present geochronologic constraints do not permit us to resolve these ambiguities. Five of the 17 sites exhibit no or minimal landslide-affected terrain in what would have been the impoundment zone upstream of the dam site: six have moderate amounts, and six have significant amounts. Based on visual estimates of how much terrain might have been affected by changes in accommodation space, we judge maximum errors on our lake volume estimates to be approximately ±50%.

Computing the Basin, Blockage, and Dimensionless Blockage indices for our dams required finding the drainage area of the channels at the blockage sites. This was determined using standard tools in ArcGIS by computing a flow accumulation raster derived from a 30-m DEM mosaic extracted to the modern drainage basin boundaries. We estimate likely errors associated with these measurements as <5%.

Computing Blockage, Dimensionless Blockage, and Impoundment indices required determining landslide dam volume, V_D. Dam volume was estimated by multiplying along-channel width by across-channel length by dam height ($W_D \times L_D \times H_D$). Because virtually all landslide dams are breached and now form part of the through-flowing channel's valley wall, most landslides have been thinned by erosion, reducing the observed vertical thickness. It is therefore difficult to estimate landslide dam thickness from the elevations of the terrain constituting the dam remnant. The H_D — the landslide height at the critical cross sections — was considered the most repeatable and consistent metric of the dam's vertical dimension. We used a second method to analyze dam thickness for comparison with the H_D estimate by considering four of the dams with distinct and easily defined planform dimensions (Dant, Warm Springs River, Burnt Ranch, and Clarno). We determined the mean elevation of channel pixels on the 10-m DEM through the reach of breached landslide. We then determined the median and 75th percentile elevations in the dam remnant, reasoning that the lower elevations in the dam remnant reflect the effects of post-dam erosion. We subtracted the mean channel elevation from the 50th and 75th percentile elevations to get two estimates of landslide dam thickness for each dam. For all four sites, both these estimates of landslide dam thickness were within 25% of H_D. In three of the four cases, H_D equaled or exceeded the other two thickness estimates. Overall, we estimate landslide dam height errors to be around ±25% and landslide dam volume errors to be at least ±50%.

To assess the morphologic effects of the landslide dams on the longitudinal profiles of the adjacent streams, we used the best available elevation data to extract the elevation values of points along an ~10–30 km channel reach bracketing each dam site. For the Heaven's Gate, Artillery, West Springs Greeley, and East Springs Greeley sites on the Owyhee

River, longitudinal profiles were extracted from a 1-m-resolution DEM based on lidar data. The channel centerline was digitized at a scale of 1:5000, based on lidar hillshades and NAIP orthophotographs. Points were constructed every 50 m along the centerline, and along-stream distances were computed for each point. Elevation values of the lidar DEM were extracted to the points. For the Whitehorse, Dant, and Wapinitia sites on the Deschutes River, a similar process was followed using DEMs derived from 2-m-resolution lidar data, with points constructed every 100 m along the channel centerline. For the Magone Lake (John Day basin) and Wolf Creek (Malheur basin) reaches, longitudinal profiles were extracted from 10-m-resolution National Elevation Data DEMs using the ArcHydro Tools add-in to ArcGIS 10. For the Warm Springs River reach (Deschutes basin); Sheep Rock, Burnt Ranch, and Clarno reaches (John Day basin); Hogsback and Deary Pasture reaches (Owyhee basin); and Chukar Park and Warm Springs Reservoir reaches (Malheur basin), profiles extracted from the DEM using automated routines produced topographic steps that were artifacts of the DEM. We therefore constructed longitudinal profiles for these reaches from contour-line intersections with the rivers as depicted on USGS 7.5-minute topographic quadrangles. Reach segments were chosen to straddle the landslide dam locations and to include enough elevation data to capture the form of the local profile; along-reach distance was determined relative to these boundaries. Benchmark and noted survey elevations were also included where appropriate. Six to eleven contour crossings or surveyed elevations were used for longitudinal profiles extracted manually. For all reaches, points falling within the breach zone of each dam site were identified in ArcGIS and marked on the longitudinal profiles.

4.2. Results

Eastern Oregon landslide dams and their inferred impoundments differ from those in other parts of the world in several ways. Landslide dams are comparable in size or smaller in Oregon. Mean dam height (H_D) is 50% lower for eastern Oregon dams than for New Zealand or worldwide dams, and dam volume (V_D) is an order of magnitude lower (Fig. 5). However, the contrast is not so great considering median values; median H_D values in Oregon are only 20–30% lower than elsewhere — a difference that is probably not significant — and median dam volumes are comparable (Fig. 5).

Another important difference relative to the potential for producing outburst floods is that the median (though not mean) impounded lake volume is larger for eastern Oregon, despite similar or smaller landslide dam volumes (Fig. 5). Mean lake length is 50% greater in eastern Oregon than worldwide, and an order of magnitude greater than in New Zealand. The differences between eastern Oregon and worldwide data are even more pronounced (500% vs. 50%) when considering median lake length.

The large volumes of the impounded lakes in eastern Oregon in part results from the larger drainage areas of channels blocked by landslide dams in our study area compared to other areas. These rivers with relatively large upstream drainage areas have lower gradients, so the landslides impound water much farther upstream. The mean and median drainage areas are, respectively, one and two orders of magnitude larger for our landslide dams than for landslide dams worldwide (Fig. 5). The mean and median drainage areas are, respectively, two and three orders of magnitude larger for our landslide dams than for New Zealand landslide dams (Fig. 5).

There is no systematic relationship between drainage area of the adjacent channel and dam volume. Dam volume spans three orders of magnitude (order 10^5–10^8) on streams with drainage areas <5000 km^2, but variability in dam volumes on rivers with drainage areas >5000 km^2 is confined to about one order of magnitude (Fig. 6).

Because of the wide range of drainage areas of channels on which landslide dams formed, the baseline gradients of the affected reaches

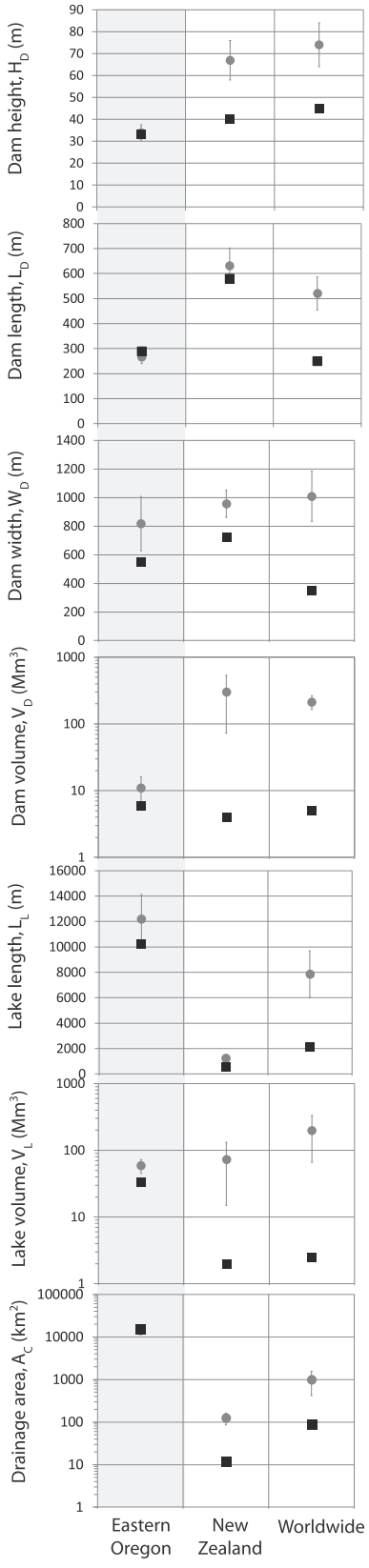

Fig. 5. Comparison of geomorphometric characteristics of eastern Oregon landslide dams with data sets from New Zealand and a worldwide compilation. New Zealand data are from Korup (2004). Drainage areas for worldwide data are from Ermini and Casagli (2003); other statistics for worldwide data are extracted from Korup (2004). Solid black squares are median values; gray circles are mean values. Standard errors on the mean are plotted. Number of dams used for statistics are 16–17 for eastern Oregon, 49–202 for New Zealand, and 83–148 for worldwide data (i.e., not all quantities were measurable or reported for each dam). Note logarithmic axes on dam volume, lake volume, and drainage area plots.

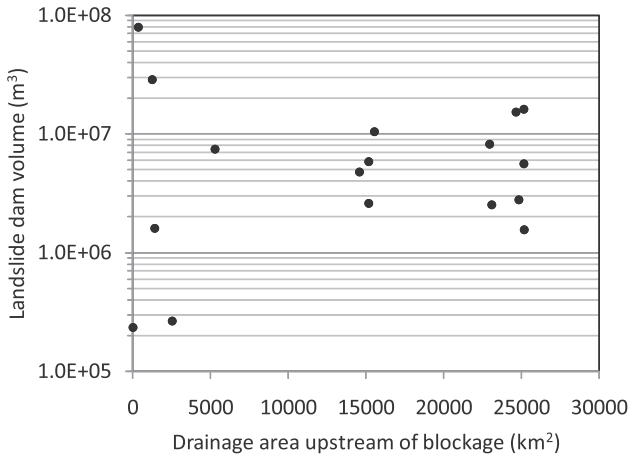

Fig. 6. Landslide dam volume plotted against drainage area upstream of blockage.

vary widely. To highlight topographic anomalies associated with landslide dams, we plotted longitudinal profiles normalized by total elevation drop and total distance along each reach (Fig. 7A) in addition to showing traditional longitudinal profiles (Fig. 7B). The longitudinal profiles of the stream reaches adjacent to the landslide dams are generally relatively linear (Fig. 7). Exceptions are the Chukar Park, Hogsback, Magone Lake, and Whitehorse dam sites, which are all at the downstream end of convexities that are several meters to several tens of meters high and extend over several hundreds of meters to several kilometers. The remaining dam sites have no systematic relationship to broad-scale profile irregularities, although most have rapids at or near the landslide dam sites.

5. Landslide dam stability indices

Morphometric characteristics of landslide dams, impounded lakes, and upstream catchments were used to compute values of five bivariate indices summarized in Korup (2004): Blockage index ($I_b = \log(V_D / A_C)$), Dimensionless Blockage index ($I_{b'} = \log(V_D / (H_D * A_C))$), Basin index ($I_a = \log({H_D}^2 / A_C)$), Impoundment index ($I_i = \log(V_D / V_L)$), and Backstow index ($I_s = \log({H_D}^3 / V_L)$). All of these indices express some formulation of dam size relative to the amount of water available to break the dam. Impoundment index and Blockage index were introduced by Casagli and Ermini (1999), while the DBI used here was introduced by Ermini and Casagli (2002). Basin index and Backstow index were introduced by Korup (2004). As noted in Section 2, all but one of the landslide dams in our study area have been breached, so we cannot use the presence of extant lakes as a criterion for *stability*, and this approach has limitations in any case (Section 1). We focus instead on whether evidence exists for catastrophic dam failure at each site, emphasizing the instability domain rather than the stability domain emphasized by others (e.g., Korup, 2004). The absence of evidence for catastrophic failure is not evidence of absence, and results must be interpreted with caution. Nonetheless, previous studies have shown that field indications of outburst flooding are often well preserved in the area (e.g., Beebee, 2003; O'Connor et al., 2003a), creating an opportunity to explore whether morphometric indices could offer a quantitative, if simple, framework for interpreting such evidence. Fig. 8 depicts the range of values for the eastern Oregon landslides relative to threshold values reported in the literature that discriminate *stable* dams from dams that failed catastrophically or breached in an unspecified fashion in other locations. For example, landslide dams considered *stable* (intact) in New Zealand have Blockage index values of >7, while landslides characterized as intact using the worldwide data set have Blockage index values of >5 (Korup, 2004; Fig. 8A). Based on New Zealand and worldwide data, breached landslide dams were found to have Blockage index values of <4 and <2, respectively.

Consistent patterns emerge from the comparison (Fig. 8A–C). First, the index values partially separating intact from breached landslide dams in the New Zealand data set (Korup, 2004) are higher than those for the dams of eastern Oregon, particularly for the Basin index (Fig. 8C). By contrast, discriminating values of Blockage index and Dimensionless Blockage index derived from worldwide data are consistent with observations in eastern Oregon. The Wolf Creek and Lake Magone sites, which lack evidence for catastrophic failure, fall into the *stable* domain; the Chukar Park site falls into the *stable* or *marginally stable* domain; and most of the rest of the sites showing evidence of catastrophic failure are within the *unstable* domain. In the field, the Chukar Park landslide dam exhibits elements of persistence and of catastrophic failure. The reach upstream of the dam site is a broad, sediment-floored valley characterized by numerous meander cutoffs in which the river's course is highly sinuous. This gives way at the dam site to a relatively straight channel full of rapids (Fig. 9). The morphology of the reach upstream of the dam site suggests that the dam itself or a topographically significant lag persisted sufficiently long, perhaps several centuries or more, for a substantial quantity of sediment to accumulate upstream. However, boulder bars along the downstream end of the landslide attest to outburst flooding from the zone we consider the most recently active part of the landslide, indicating at least partial cataclysmic breaching. This multipronged (and multifaceted) landslide character is common to several other eastern Oregon landslides (e.g., West Springs Greeley, Warm Springs Reservoir) and complicates dam stability analysis.

Along with the Chukar Park dam site, the Whitehorse, Hogsback, and Magone Lake dam sites also show evidence of perturbing the longitudinal profiles of local stream reaches (Fig. 7). However, these sites do not all occupy the same region on the bivariate plots. The Whitehorse and Hogsback dams fall within the *unstable* domains of the Blockage, Basin, and Dimensionless Blockage index plots, while Magone Lake and Chukar Park do not. In the field, the Hogsback site lacks evidence of upstream sediment accumulation. Terraces do occur upstream from the Whitehorse dam site, but the sediment accumulation is not nearly as extensive as upstream from the Chukar Park site.

Two sites, Warm Springs River and Hogsback, whose downstream reaches we were unable to observe in the field, plot in *unstable* domains of the Basin index, Blockage index, and Dimensionless Blockage index graphs (Fig. 8A–C). This result constitutes a prediction that can be tested if we gain access to those sites. One site, Wapinitia, shows no clear field evidence of catastrophic dam failure and also plots in the *unstable* region of these graphs. At Wapinitia, another landslide complex impinges on the channel immediately downstream of the dam site, possibly covering or obliterating outburst flood deposits from breaching of the Wapinitia landslide. The downstream landslide complex, which gives rise to Boxcar Rapids on the Deschutes River, is judged by Beebee (2003) to be younger than Wapinitia, based on apparent freshness of slide mass morphology, and auger data are consistent with this observation (Section 3). However, if we take the field evidence at face value, the Basin, Blockage, and Dimensionless Blockage indices all mischaracterize the Wapinitia site as being susceptible to catastrophic failure.

The Impoundment index cleanly separates the landslide dams that do and do not exhibit evidence for catastrophic failure (Fig. 8D). However, the discriminating value is −0.7, rather than 0 for worldwide data or 1 for New Zealand data. The Hogsback site is predicted not to have failed catastrophically, according to this value.

The Backstow index is the poorest at discriminating eastern Oregon dam sites with and without evidence of catastrophic dam failure (Fig. 8E). Index values for the *stable* and *unstable* dams substantially overlap. The threshold value for *stable* dams in New Zealand lies far above those from our sites, and the threshold for *unstable* dams runs through the middle of the eastern Oregon observations (Fig. 8E).

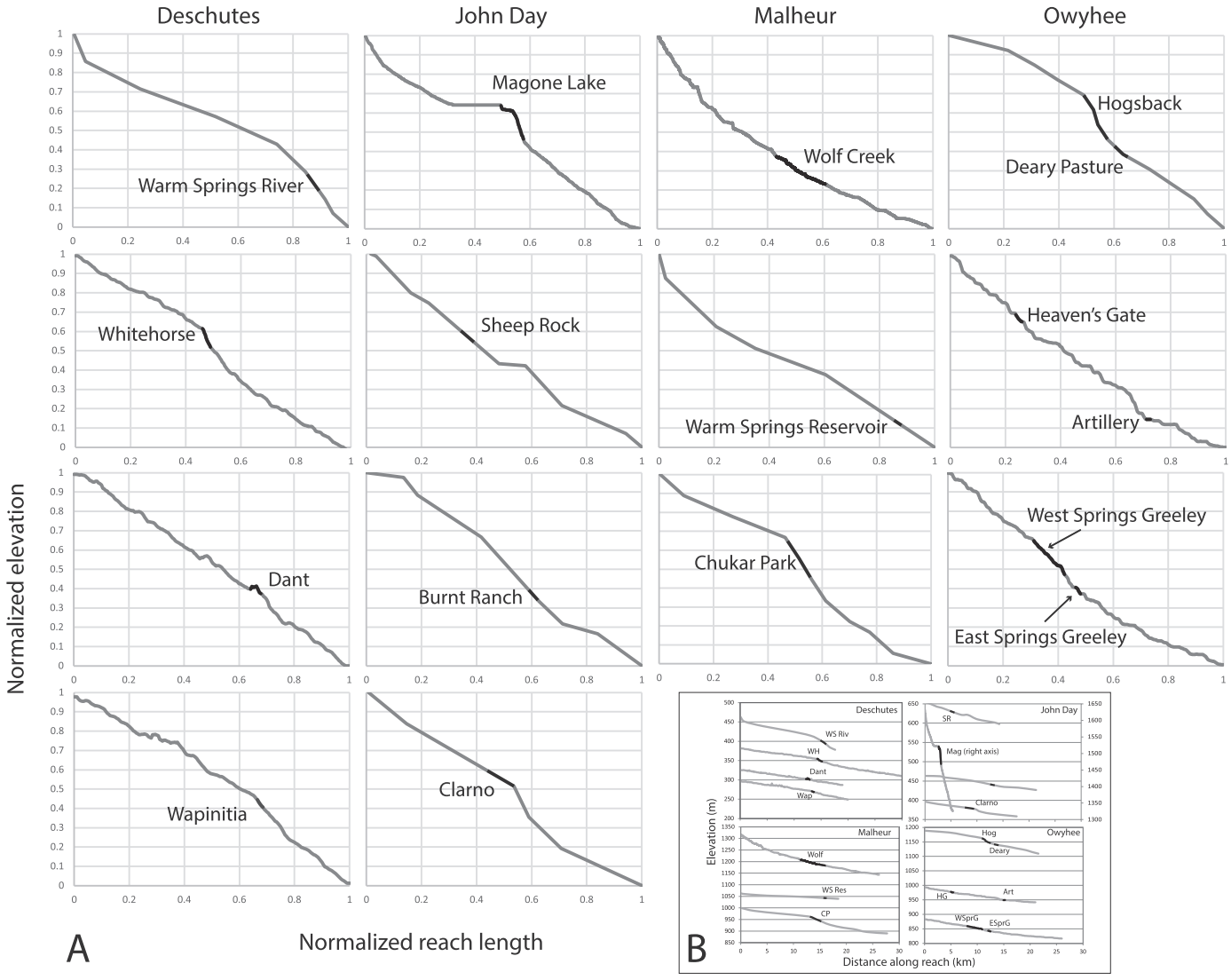

Fig. 7. Longitudinal profiles of stream reaches straddling landslide dam study sites. Black lines indicate segments of the profiles that cut through landslide dams. Profiles containing Whitehorse, Dant, Wapinitia, Heaven's Gate, Artillery, West Springs Greeley, and East Springs Greeley sites are derived from lidar data; profiles containing Magone Lake and Wolf Creek were extracted from National Elevation Data set 10-m DEMs; all other profiles were constructed from points where contours on 1:24,000 USGS digital topographic quadrangles crossed the study stream reaches. See Section 4.1 for details. (A) Profiles normalized by total elevation drop and distance along reach. (B) Standard longitudinal profiles. Note the dual y-axes on John Day graph: Right-hand axis pertains to Magone Lake profile; left-hand axis pertains to all other profiles. Abbreviations: WS Riv = Warm Springs River; WH = Whitehorse; Wap = Wapinitia; SR = Sheep Rock; Mag = Magone Lake; Wolf = Wolf Creek; WS Res = Warm Springs Reservoir; CP = Chukar Park; Hog = Hogsback; Deary = Deary Pasture; HG = Heaven's Gate; Art = Artillery; WSprG = West Springs Greeley; ESprG = East Springs Greeley.

6. Discussion

Overall, most of the ancient dam sites we analyzed in eastern Oregon appear to have been unstable. Only three of the 17 sites with channel-blocking landslides lack evidence for catastrophic outburst flooding. Fig. 10 illustrates an example of such field evidence.

The percentage (82%) of dams in eastern Oregon that failed catastrophically exceeds the 45 to 70% (depending on materials involved) reported for worldwide data (Ermini and Casagli, 2002) and the 37% of *unstable* dams in New Zealand (Korup, 2004). Field evidence for widespread catastrophic failure of eastern Oregon landslide dams is consistent with the implications of landslide dam stability indices, given the morphometric character of the region's landslide dams and their impoundments. The ratio of dam size to impoundment size is smaller in eastern Oregon than for other settings (Fig. 5), and broadly speaking, smaller ratios promote instability as predicted by the indices.

A complication of our analysis is that the landslide complexes that generate dams in eastern Oregon are in some cases many square kilometers in extent, yet the dams themselves are commonly formed by only a small finger of landslide material. The most striking example of this is the Warm Springs Reservoir site, which has the largest landslide complex area (39.6 km^2) and one of the smallest landslide dam volumes (264,600 m^3) in our data set. The dynamics of these landslide complexes are not well understood, but some of them appear to be progressive (Othus, 2008; Safran et al., 2011; Markley, 2013). While some of the region's landslide complexes have clearly persisted for many tens of thousands of years (Safran et al., 2011), in most cases, the whole slide mass is not active at any one time (Othus, 2008; Markley, 2013). Field evidence of channel damming and of dam breaching likely relates only to the most recent blockage or blockages. The length scale of a dam might be set by the dominant topographic wavelengths in the landslide mass, which in turn may depend on landslide type and material. Along portions of the Owyhee River, for example, failure slices in multiple rotational complexes are typically spaced several tens to ~100 m apart (Safran et al., 2011; Markley, 2013). The impingement of these blocks on the channel at an angle helps to set the scale of the

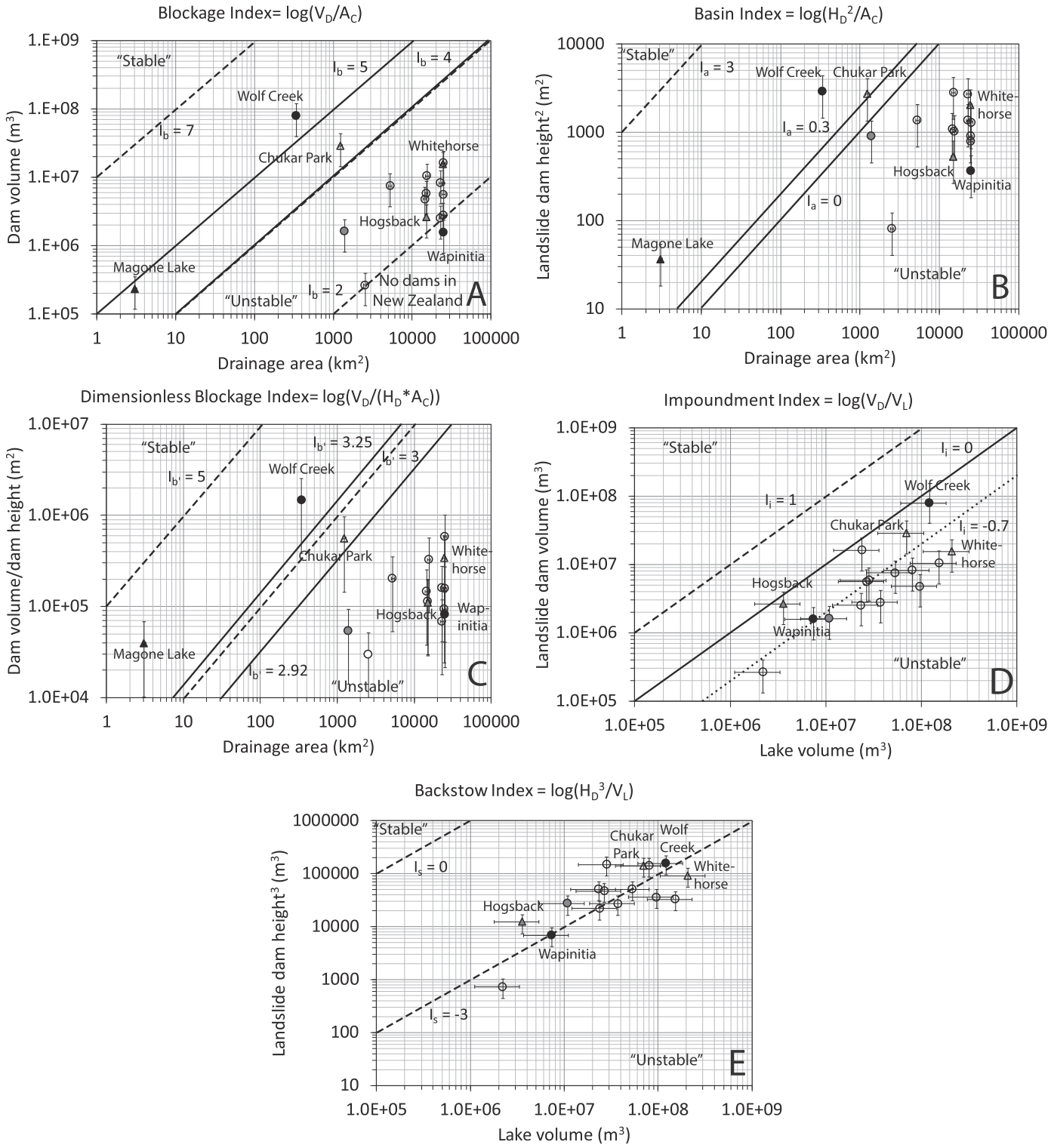

Fig. 8. Morphometric index values, computed from measured characteristics of landslide dams, impounded lakes, and upstream catchments. Size of error bars reflect estimated error in measured quantities (Section 4.1), which were propagated through derived quantities (e.g., $H_D \times A_C$). Lines show threshold index values separating dams that were deemed *stable* vs. *unstable* in various localities (Ermini and Casagli, 2003; Korup, 2004). Meaning of *stable* and *unstable* designations is explained in Section 1. Solid lines: Worldwide data (Ermini and Casagli, 2003; Korup, 2004). Dashed lines: New Zealand (Korup, 2004). Dotted line, fitted by eye (panel D only): eastern Oregon. Open circles are dams exhibiting evidence of outburst flooding. Gray circles are dam sites downstream of which we lack field observations. Solid black circles are dams exhibiting no evidence of outburst flooding and are labeled with site names, as are triangles: dam sites associated with knickpoints.

along-channel dam dimension, typically on the order of several hundreds of meters. We are currently working to better quantify and identify the controls on intraslide topography in eastern Oregon (Markley, 2013).

In contrast to relatively small landslide dam volumes, the lake volumes and/or upstream catchment areas of dammed channels are relatively large in eastern Oregon. Large impoundments result from the low regional gradients that characterize this plateau environment.

Fig. 9. Oblique Google Earth image of Chukar Park landslide dam site. North Fork Malheur River flows from top to bottom of image. A pair of landslide complexes, outlined in white, flank the river on both sides. Based on field observations, the landslide dam crest is believed to be along the short, valley-perpendicular line, and the breach zone is spanned by the long, valley-parallel line.

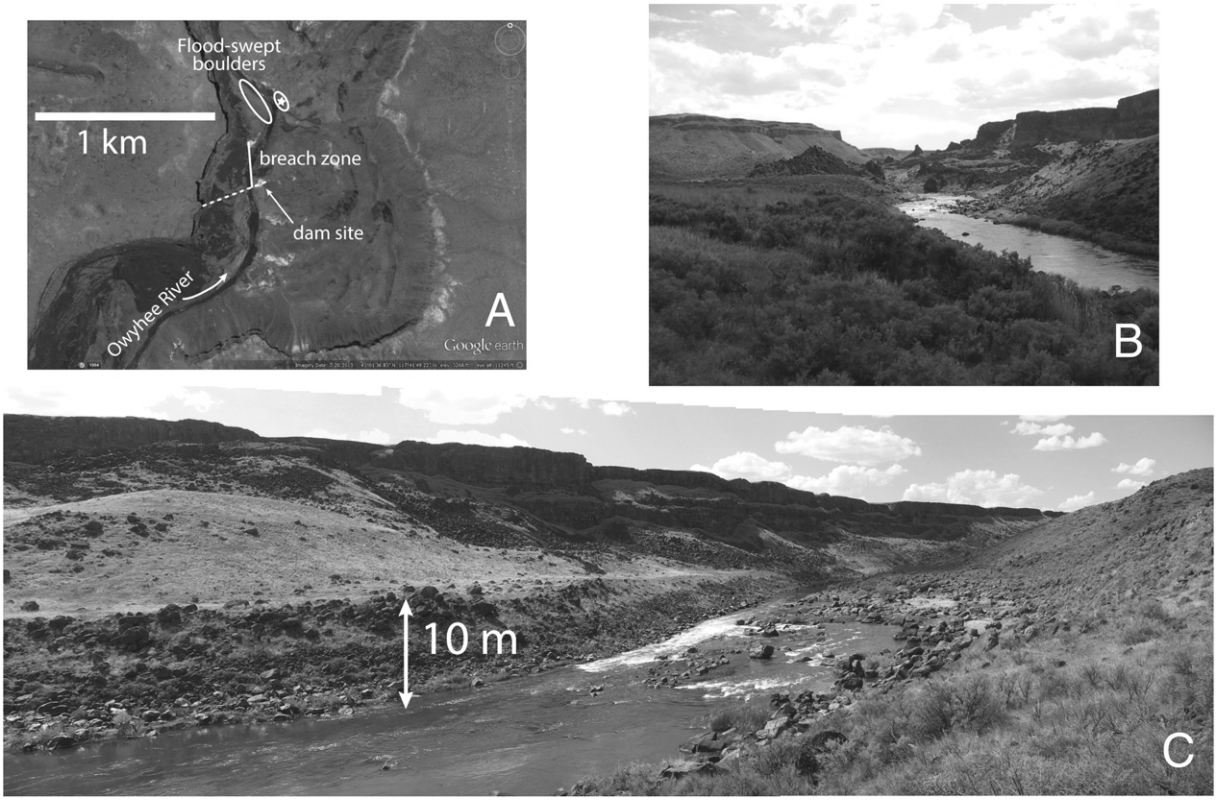

Fig. 10. Field evidence for outburst flooding, Artillery landslide reach. (A) Artillery landslide complex, illustrating location of critical cross-section at dam site (dashed line; near location of Fig. 3), breach zone (solid line), and terraces capped by flood-swept boulders (ellipses). Star marks location from which photos in (B) and (C) were taken. Image from Google Earth. (B) View upstream toward dam site. (C) Panoramic view across valley and downstream.

Low channel gradients (predominantly 0.002–0.005, except near Magone Lake: ~0.04) result in long lakes on the order of 10 km (Fig. 5). Lake volumes are also enhanced by the large landslide complexes themselves, which widen valleys by locally reducing valley wall gradients to 8–14° (Safran et al., 2011).

The large drainage areas of the channels at our dam sites are a function of the dominant regional controls on landslide occurrence. In a landslide distribution analysis, Safran et al. (2011) showed that eastern Oregon landslides are preferentially localized where coherent, typically volcanic, rocks overlie weak, typically fluviolacustrine or volcaniclastic units, along escarpments and canyon walls. The distribution of the key contacts that promote landsliding is established by the volcanic and tectonic history of the region and is largely independent of geomorphic controls; these key contacts can outcrop anywhere along a channel network. At the same time, the relief to drive landsliding is largely confined to tectonic or volcanic escarpments or to the walls of canyons. Although only modest local relief (~100 m) is required to drive mass movement where key contacts are exposed (Safran et al., 2011), in this relatively low relief environment characterized by accumulation of volcaniclastic and volcanic deposits since at least Miocene times, such exposures are most common along major rivers. Thus, the conditions for landslide dam formation are commonly met on channels with large drainage areas. This distinguishes the eastern Oregon landscape from montane settings in which topographic gradients dominate large landslide distributions (Korup et al., 2007). In such mountainous settings, the steepest and most landslide-prone slopes may be in headwater areas with relatively low drainage areas. Because in eastern Oregon landslide dam volume does not increase systematically with drainage area of the adjacent channel (Fig. 6), conditions for catastrophic dam failure can likewise occur throughout these large basins.

Landslides on high-order channels potentially disrupt fluvial architecture (Korup and Crozier, 2002) and longitudinal profile evolution (Ouimet et al., 2007; Safran et al., 2008). However, significant inhibition of valley incision over timescales of 10^6 years requires repeated and relatively persistent (e.g., 10^3–10^4 years) landslide dams, dam remnants, or upstream sediment accumulations that create channel "plugs" (Safran et al., 2008). There is no timescale associated with morphometry-based dam stability assessments. Based on historical data, Costa and Schuster (1988, 1991) reported that 85% of landslide dams that fail do so within a year of formation, but many landslide dams do not fail. Moreover, Hewitt (1998), Ermini and Casagli (2002), and Hermanns et al. (2006, 2011a) noted that landslide dam stability for hundreds or even thousands of years does not preclude the possibility of ultimate catastrophic failure.

Complex landslide and flood histories have been documented in individual instances around the world (e.g., Hewitt, 1998; Hermanns et al., 2004, 2006, 2009, 2011a), but the relative importance of various controls on dam longevity remain uncertain. Some emphasize the importance of lithologic and geotechnical properties of dams, such as grain size or degree of fragmentation, on dam persistence (Ermini and Casagli, 2002; Casagli et al., 2003; Davies and McSaveney, 2006; Dunning and Armitage, 2011). Others highlight time-dependent controls on dam integrity, such as the interplay between three-dimensional dam morphology and the surrounding bedrock (Dunning et al., 2005; Hermanns et al., 2009, 2011b); climatic variability (Hermanns et al., 2004, 2011a); and individual hydrologic and mass-wasting events affecting dams or their associated impoundments (Hermanns et al., 2004, 2011a).

Although none of the eastern Oregon landslide dams have sufficient absolute age information to determine their persistence, about half of the dam sites we studied possibly have upstream sediment accumulations (Table 1). This implies at least some period of landslide dam stability prior to breaching. In most cases, however, breaching was at least partly catastrophic, leaving downstream evidence of flooding. Only impoundments not completely filled with sediment could produce such flooding.

Even short-lived landslide dams or incomplete valley occlusions can have local impacts on longitudinal profiles. Four of the eastern Oregon dam sites appear spatially associated with some sort of convexity in the longitudinal profile of the channel upstream of the dam site (Fig. 7), although only the knickpoint at Whitehorse is depicted in detail with high-resolution topographic data. As noted in Section 3, the Magone Lake, Chukar Park, and Hogsback dam sites are known (Magone Lake) or suspected to be of Holocene age, possibly post-dating the Mazama eruption, which may help explain the relative prominence of the associated knickpoints, although the Whitehorse dam is likely older (Section 3). Perturbations associated with landslide dams do not appear to govern the overall form of the longitudinal profile as seen, for example, by Ouimet et al. (2007) in landslide-affected reaches in eastern China. Modeling of the morphologic consequences of landslide dam-related incision inhibition suggests that those more significant impacts on the longitudinal profile, which include long-wavelength (tens of kilometers) convexities with amplitudes of hundreds of meters, require spatial clustering of landslides, long-term persistence of landslide dams relative to the rate of base-level lowering, and few floods capable of mobilizing large landslide lag material or incising into bedrock (Safran et al., 2008). In some cases, dam-failure floods are the only flows capable of moving large in-channel landslide debris (Beebee, 2003) that localizes knickpoints. Reactivation of individual landslide complexes is commonplace, and in eastern Oregon multiple dams may be generated over time at a single site or along a channel reach (e.g., Othus, 2008; Safran et al., 2011). However, despite landslide-related features that dominate the geomorphic character of some channel reaches in the region for thousands of years (e.g., O'Connor et al., 2003a), there is little evidence thus far that the ancient landslide dams in eastern Oregon control the longer-term, million-year-timescale evolution of longitudinal profiles by forming lasting plugs.

Landslide dam stability assessments based on morphometric indices offer a blunt but simple tool for characterizing the relative propensity for dams in a given environment to fail. They are subject to error because they neglect a variety of important controls, including those described above. Nonetheless, this study indicates that the functional form, and in some cases even the threshold values, of several morphometric indices are applicable to landslide dams in this semiarid, low-relief environment. The threshold values of Blockage and Dimensionless Blockage indices calibrated to worldwide data appear most applicable to the eastern Oregon data, perhaps because of the diverse range of environments these data sets include. The threshold values of the Blockage and Impoundment indices calibrated to the Apennines are higher than the thresholds applicable to the eastern Oregon data.

The threshold values derived from the New Zealand data are the highest of all and do not appear to have predictive value for the landslide dams of eastern Oregon. For a given metric of water available for dam breaching (e.g., upstream catchment area or lake volume), dam volumes must be several orders of magnitude greater to be stable in New Zealand than in eastern Oregon. Korup (2004) speculated that the stability of dams in New Zealand may be limited by rapid rates of surface erosion related to earthquakes and the abundance of high-intensity rainstorms. Geotechnical properties of landslide dams may also differ between the two regions, such as material size, sorting, and compaction, which themselves might relate to landslide type (e.g., rockfall vs. earthflow) and lithologic controls. Further work is required to explore these linkages systematically.

7. Conclusion

The stability of landslide dams can mediate the effects of hillslope form and processes on fluvial incision and therefore on regional landscape evolution. Eastern Oregon is a relatively dry, low-relief, primarily extensional, continental interior landscape. This tectonic setting promotes stratigraphic sequences, in particular lava flows capping

fluviolacustrine and volcaniclastic sediments, prone to landsliding along river corridors of diverse drainage areas. The blocky or modular character of many of the region's landslides produces dams that are small relative to the area of entire landslide complexes. Low regional gradients lead to large water impoundments. Previously developed bivariate indices of landslide stability suggest that a small ratio of dam volume to water available for dam breaching, as found in eastern Oregon, promotes catastrophic dam failure. Such failures are indicated by flood deposits downstream of most of the dam sites studied. While the landslide dams of eastern Oregon may temporarily serve as channel plugs, their general instability implies that they are primarily flood-makers. Future research on the effects of repeated outburst flooding on long-term incision rates is needed.

Acknowledgments

This work was funded by the Geological Society of America's Gladys Cole Award; National Science Foundation grant EAR-617347; and the John S. Rogers Summer Internship Program at Lewis & Clark College. Owyhee River lidar topographic data were obtained through the National Center for Airborne Laser Mapping (NCALM); acquisition was partially funded by an NCALM seed grant. Funding sources had no role in study design; collection, analysis, and interpretation of data; writing of this manuscript; or the decision to submit this work for publication. Dylan Peden and Chris Scheffler provided field assistance. JoJo Mangano and Miranda Wood facilitated stream profile extraction from lidar and USGS topographic quads. The Bureau of Land Management and local landowners granted access and logistical assistance. We thank Oliver Korup and Richard Marston for the time and effort they devoted in helping us improve this manuscript for publication. Any use of trade, firm, or product names is for descriptive purposes only and does not imply endorsement by the U.S. Government.

Appendix A. Supplementary data

Supplementary data to this article can be found online at http://dx.doi.org/10.1016/j.geomorph.2015.06.040.

References

Beebee, R.A., 2003. Snowmelt Hydrology, Paleohydrology, and Landslide Dams in the Deschutes River Basin, Oregon (Ph.D. Dissertation) University of Oregon, Eugene.
Beranek, L.P., Link, P.K., Fanning, C.M., 2006. Miocene to Holocene landscape evolution of the western Snake River Plain region, Idaho: using the SHRIMP detrital zircon provenance record to track eastward migration of the Yellowstone hotspot. Geol. Soc. Am. Bull. 118, 1027–1050. http://dx.doi.org/10.1130/B25896.1.
Burchsted, D., Daniels, M., Wohl, E.E., 2014. Introduction to the special issue on discontinuity of fluvial systems. Geomorphology 205, 1–4. http://dx.doi.org/10.1016/j.geomorph.2013.04.004.
Camp, V.E., Ross, M.E., 2004. Mantle dynamics and genesis of mafic magmatism in the intermontane Pacific Northwest. J. Geophys. Res. 109, B08204. http://dx.doi.org/10.1029/2003JB002838.
Carter, D.T., Ely, L.L., O'Connor, J.E., Fenton, C.R., 2006. Late Pleistocene outburst flooding from pluvial Lake Alvord into the Owyhee River, Oregon. Geomorphology 75, 346–367.
Casagli, N., Ermini, L., 1999. Geomorphic analysis of landslide dams in the Northern Apennines. Trans. Jpn. Geomorphol. Union 20 (3), 219–249.
Casagli, N., Ermini, L., Rosati, G., 2003. Determining grain size distribution of the materials composing landslide dams in the Northern Apennines: sampling and processing methods. Eng. Geol. 69, 83–97.
Christiansen, R.L., Yeats, R.S., 1992. Post-Laramide geology of the U. S. Cordilleran region. In: Burchfiel, B.C., Lipman, P.W., Zoback, M.L. (Eds.), The Cordilleran Orogen; Conterminous U.S. Decade of North American Geology vol. G-3. Geological Society of America, Denver, CO, pp. 261–406.
Costa, J.E., Schuster, R.L., 1988. The formation and failure of natural dams. Geol. Soc. Am. Bull. 100, 1054–1068.
Costa, J.E., Schuster, R.L., 1991. Documented historical landslide dams from around the world. U. S. Geological Survey Open-File Report, pp. 91–239.
Cummings, M.L., 1991. Geology of the Deer Butte Formation, Malheur County, Oregon; faulting, sedimentation and volcanism in a post-caldera setting. Sediment. Geol. 74, 345–362.
Cummings, M.L., Evans, J.G., Ferns, M.L., Lees, K.R., 2000. Stratigraphic and structural evolution of the middle Miocene synvolcanic Oregon–Idaho graben. Geol. Soc. Am. Bull. 112, 668–682.
Davies, T.R., McSaveney, M.J., 2006. Dynamic fragmentation in landslides: application to natural dam stability. Ital. J. Eng. Geol. Environ. Special Issue I, 123–126. http://dx.doi.org/10.4408/IJEGE:2006-01.S-16.
Dunning, S.A., Armitage, P.J., 2011. The grain-size distribution of rock-avalanche deposits: implications for natural dam stability. In: Evans, S.G., Hermanns, R.L., Strom, A., Scarascia-Mugnozza, G. (Eds.), Natural and Artificial Rockslide DamsLecture Notes in Earth Sciences vol. 133. Springer Berlin Heidelberg, pp. 479–498. http://dx.doi.org/10.1007/978-3-642-04764-0_19.
Dunning, S., Petley, D., Rosser, N., Strom, A., 2005. The morphology and sedimentology of valley confined rock-avalanche deposits and their effect on potential dam hazard. In: Hungr, O., Fell, R., Couture, R., Eberhardt, E. (Eds.), Landslide Risk Management. Taylor and Francis Group, London, pp. 691–701.
Ely, L.E., Brossy, C.C., House, P.K., Safran, E.B., O'Connor, J.E., Champion, D.E., Fenton, C.R., Bondre, N.R., Orem, C.A., Grant, G.E., Henry, C.D., Turin, B.D., 2012. Owyhee River intracanyon lava flows: does the river give a dam? Geol. Soc. Am. Bull. 124, 1667–1687. http://dx.doi.org/10.1130/B30574.1.
Ermini, L., Casagli, N., 2002. Criteria for a preliminary assessment of landslide dam evolution. In: Rybar, J., Sternbeck, J., Wagner, P. (Eds.), Landslides. Proceedings 1st European Conference on Landslides 24–26 June 2002, Prague, Balkema, pp. 157–162.
Ermini, L., Casagli, N., 2003. Prediction of the behavior of landslide dams using a geomorphical dimensionless index. Earth Surf. Process. Landf. 28, 31–47.
Hermanns, R.L., Niedermann, S., Ivy-Ochs, S., Kubik, P.W., 2004. Rock avalanching into a landslide-dammed lake causing multiple dam failure in Las Conchas valley (NW Argentina) — evidence from surface exposure dating and stratigraphic analyses. Landslides 1, 113–122. http://dx.doi.org/10.1007/s10346-004-0013-5.
Hermanns, R.L., Folguera, A., Gonzales Diaz, F.E., Fauque, L., 2006. Landslide dams in the Central Andes of Argentina — showing the need of revising the established landslide dam classification. Ital. J. Eng. Geol. Environ. Special Issue I, 55–60. http://dx.doi.org/10.4408/IJEGE:2006-01.S-06.
Hermanns, R.L., Blikra, L.H., Longva, O., 2009. Relation between rockslide dam and valley morphology and its impact on rockslide dam longevity and control on potential breach development based on examples from Norway and the Andes. In: Bauer, E., Semprich, S., Zenz, G. (Eds.), Long Term Behavior of Dams: Proceedings of the 2nd International Conference. Verlag der Technischen Universität Graz, Graz, pp. 789–794.
Hermanns, R.L., Folguera, A., Penna, I., Fauque, L., Niedermann, S., 2011a. Landslide dams in the Central Andes of Argentina (Northern Patagonia and the Argentine Northwest). In: Evans, S.G., Hermanns, R.L., Strom, A., Scarascia-Mugnozza, G. (Eds.), Natural and Artificial Rockslide DamsLecture Notes in Earth Sciences vol. 133. Springer Berlin Heidelberg, pp. 147–176.
Hermanns, R.L., Hewitt, K., Strom, A., Evans, S.G., Dunning, S.A., Scarascia-Mugnozza, G., 2011b. The classification of rockslide dams. In: Evans, S.G., Hermanns, R.L., Strom, A., Scarascia-Mugnozza, G. (Eds.), Natural and Artificial Rockslide DamsLecture Notes in Earth Sciences vol. 133. Springer Berlin Heidelberg, pp. 581–593.
Hewitt, K., 1998. Catastrophic landslides and their effects on the Upper Indus streams, Karakoram Himalaya, northern Pakistan. Geomorphology 26, 47–80.
Hewitt, K., 2006. Disturbance regime landscapes: mountain drainage systems interrupted by large rockslides. Prog. Phys. Geogr. 30, 365–393. http://dx.doi.org/10.1191/0309133306pp486ra.
Hewitt, K., Clague, J.J., Orwin, J.F., 2008. Legacies of catastrophic rock slope failures in mountain landscapes. Earth-Sci. Rev. 87, 1–38.
Hewitt, K., Gosse, J., Clague, J.J., 2011. Rock avalanches and the pace of late Quaternary development of river valleys in the Karakorum Himalaya. Geol. Soc. Am. Bull. 123, 1836–1850.
Ibarra, D.E., Egger, A.E., Weaver, K.L., Harris, C.R., Maher, K., 2014. Rise and fall of late Pleistocene pluvial lakes in response to reduced evaporation and precipitation: evidence from Lake Surprise, California. Geol. Soc. Am. Bull. 126, 1387–1415. http://dx.doi.org/10.1130/B31014.1.
Korup, O., 2002. Recent research on landslide dams; a literature review with special attention to New Zealand. Prog. Phys. Geogr. 26, 206–235.
Korup, O., 2004. Geomorphic characteristics of New Zealand landslide dams. Eng. Geol. 73, 13–35.
Korup, O., 2005. Large landslides and their effect on sediment flux in South Westland, New Zealand. Earth Surf. Process. Landf. 30, 305–323. http://dx.doi.org/10.1002/esp.1143.
Korup, O., 2006. Rock-slope failure and the river long profile. Geology 34, 45–48.
Korup, O., 2011. Rockslide and rock avalanche dams in the Southern Alps, New Zealand. In: Evans, S.G., Hermanns, R.L., Strom, A., Scarascia-Mugnozza, G. (Eds.), Natural and Artificial Rockslide DamsLecture Notes in Earth Sciences vol. 133. Springer Berlin Heidelberg, pp. 123–145.
Korup, O., Crozier, M., 2002. Landslide types and geomorphic impact on river channels, Southern Alps, New Zealand. In: Rybar, J., Sternbeck, J., Wagner, P. (Eds.), Landslides. Proceedings 1st European Conference on Landslides 24–26 June 2002, Prague, Balkema, pp. 233–238.
Korup, O., Strom, A.L., Weidinger, J.T., 2006. Fluvial response to large rock-slope failures: examples from the Himalayas, the Tien Shan, and the Southern Alps in New Zealand. Geomorphology 78, 3–21.
Korup, O., Clague, J.J., Hermanns, R.L., Hewitt, K., Strom, A.L., Weidinger, J.T., 2007. Giant landslides, topography, and erosion. Earth Planet. Sci. Lett. 261, 578–589.
Korup, O., Densmore, A.L., Schlunegger, F., 2010. The role of landslides in mountain range evolution. Geomorphology 120, 77–90. http://dx.doi.org/10.1016/j.geomorph.2009.09.017.
Markley, C., 2013. Characterization of mass wasting through the spectral analysis of LiDAR imagery: Owyhee River, southeastern Oregon (M.S. thesis) Central Washington University, Ellensburg.
Mosgrove, J.L., 1980. The Malheur National Forest: An Ethnographic History. USDA Forest Service, Pacific Northwest Region, Portland, U.S.A.

O'Connor, J.E., Beebee, R.A., 2009. Floods from natural rock-material dams. In: Burr, D., Carling, P., Baker, V. (Eds.), Megafloods on Earth and Mars. Cambridge University Press, Cambridge, U.K., pp. 128–171.
O'Connor, J.E., Grant, G.E. (Eds.), 2003. A peculiar river, the geology and geomorphology of the Deschutes River, Oregon. American Geophysical Union Water Science and Application Series No. 7, Washington, DC (219 pp.).
O'Connor, J.E., Curran, J.H., Beebee, R.A., Grant, G.E., Sarna-Wojcicki, A., 2003a. Quaternary geology and geomorphology of the lower Deschutes River canyon, Oregon. In: O'Connor, J.E., Grant, G.E. (Eds.), A Peculiar River—Geology, Geomorphology, and Hydrology of the Deschutes River, Oregon. American Geophysical Union Water Science and Application Series No. 7, Washington, DC, pp. 73–94.
O'Connor, J.E., Grant, G.E., Haluska, T.L., 2003b. Overview of geology, hydrology, geomorphology, and sediment budget of the Deschutes River basin, Oregon. In: O'Connor, J.E., Grant, G.E. (Eds.), A Peculiar River—Geology, Geomorphology, and Hydrology of the Deschutes River, Oregon. American Geophysical Union Water Science and Application Series No. 7, Washington, DC, pp. 7–29.
O'Connor, J.E., Clague, J.J., Walder, J.S., Manville, V., Beebee, R.A., 2013. Outburst Floods. In: Shroder, J. (Editor in Chief), Wohl, E.E., (Ed.), Treatise on Geomorphology, v. 9 (Fluvial Geomorphology). Academic Press, San Diego, U.S.A., pp. 475–510.
Oster, J.L., Ibarra, D.E., Winnick, M.J., Maher, K., 2015. Steering of westerly storms over western North America at the Last Glacial Maximum. Nat. Geosci. 8, 201–205. http://dx.doi.org/10.1038/NGEO2365.
Othus, S.M., 2008. Comparison of Landslides and Their Related Outburst Flood Deposits, Owyhee River, Southeastern Oregon (M.S. Thesis) Central Washington University, Ellensburg.
Ouimet, W.B., Whipple, K.X., Royden, L.H., Sun, Ziming, Chen, Ziliang, 2007. The influence of large landslides on river incision in a transient landscape: eastern margin of the Tibetan Plateau (Sichuan, China). Geol. Soc. Am. Bull. 119, 1462–1476.
Philip, H., Ritz, J.-F., 1999. Gigantic paleolandslide associated with active faulting along the Bogd fault (Gobi-Altay, Mongolia). Geology 27, 211–214.
Reneau, S.L., Dethier, D.P., 1996. Late Pleistocene landslide-dammed lakes along the Rio Grande, White Rock Canyon, New Mexico. Geol. Soc. Am. Bull. 108, 1492–1507.
Repenning, C.A., Weasma, T.R., Scott, G.R., 1995. The early Pleistocene (latest Blancan–earliest Irvingtonian) Froman Ferry fauna and history of the Glenns Ferry Formation, southwestern Idaho. U.S. Geol. Surv. Bull. 2105.
Safran, E.B., Peden, J.D., Harrity, K., Anderson, S.W., O'Connor, J.E., Wallick, R., House, P.K., Ely, L., 2008. Impacts of landslide dams on river profile evolution. EOS Trans. Am. Geophys. Union 89 (53) (Fall Meeting Supplement, Abstract H54D-03).
Safran, E.B., Anderson, S.W., Mills-Novoa, M., House, P.K., Ely, L., 2011. Controls on large landslide distribution and implications for the geomorphic evolution of the southern interior Columbia River basin. Geol. Soc. Am. Bull. 123, 1851–1862.
Schuster, R.L., 2006. Impact of landslide dams on mountain valley morphology. In: Evans, S.G., Hermanns, R.L., Strom, A., Scarascia-Mugnozza, G. (Eds.), Natural and Artificial Rockslide DamsLecture Notes in Earth Sciences vol. 133. Springer Berlin Heidelberg, pp. 591–616.
Smith, G.A., 1986. Simtustus Formation: Paleogeographic and stratigraphic significance of a newly defined Miocene unit in the Deschutes basin, central Oregon. Or. Geol. 48, 63–72.
van Gorp, W., Temme, J.A.M., Baartman, J.E.M., Schoorl, J.M., 2014. Landscape evolution modeling of naturally dammed rivers. Earth Surf. Process. Landf. 39, 1587–1600. http://dx.doi.org/10.1002/esp.3547.
Van Tassell, J., Ferns, M., McConnell, V., Smith, G.R., 2001. The mid-Pliocene Imbler fish fossils, Grande Ronde Valley, Union County, Oregon, and the connection between Lake Idaho and the Columbia River. Or. Geol. 63, 77–84 (and 89–96).
Walsh, L.S., Martin, A.J., Ojha, T.P., Fedenczuk, T., 2012. Correlations of fluvial knickzones with landslide dams, lithologic contacts, and faults in the southwestern Annapurna Range, central Nepalese Himalaya. J. Geophys. Res. 117, F01012. http://dx.doi.org/10.1029/2011JF001984.
Whipple, K.X., Tucker, G.E., 1999. Dynamics of the stream-power river incision model: Implications for height limits of mountain ranges, landscape response time-scales, and research needs. J. Geophys. Res. 104 (B8), 17,661–17,674.